Nanotubes from Carbon

P. M. Ajayan

Department of Materials Science & Engineering, Rensselaer Polytechnic Institute, Troy, New York 12180-3590

Received June 29, 1998 (Revised Manuscript Received March 4, 1999)

Contents

I. Nanotubular Carbon

It is the chemical genius of carbon that it can bond in different ways to create structures with entirely different properties. Graphite and diamond, the two bulk solid phases of pure carbon, bear testimony to this. The mystery lies in the different hybridization that carbon atoms can assume. The four valence electrons in carbon, when shared equally (sp^3 hybridized), create isotropically strong diamond. But when only three are shared covalently between neighbors in a plane and the fourth is allowed to be delocalized among all atoms, the resulting material is graphite. The latter (sp^2) type of bonding builds a layered structure with strong in-plane bonds and weak out-of-plane bonding of the van der Waals type. Graphite, hence, is weak normal to its planes and is considered as a soft material due to its ability to slide along the planes. The story of fullerenes and nanotubes[1] belongs to the architecture of sp^2 bonded carbon and the subtlety of a certain group of topological defects that can create unique, closed shell structures out of planar graphite sheets.

Graphite is the thermodynamically stable bulk phase of carbon up to very high temperatures under normal ranges of pressure (diamond is only kinetically stable). It is now well known that this is not the case when there are only a finite number of carbon atoms. Simply speaking, this has to do with the high density of dangling bond atoms when the size of the graphite crystallites becomes small (say, nanosize). At small sizes, the structure does well energetically by closing onto itself and removing all the dangling bonds. Preliminary experiments done in the mid 1980s,[2] which served as the precursor to the fullerene discovery,[3] suggested that when the number of carbon atoms is smaller than a few hundred, the structures formed correspond to linear chains, rings, and closed shells. The latter, called fullerenes, are closed shell all carbon molecules with an even number of atoms (starting at C_{28}, which has been observed by mass spectrometers in carbon soot) and nominal sp^2 bonding between adjacent atoms.

Professor Ajayan received his Ph.D. in materials science and engineering from Northwestern University in 1989. He spend three years of post-doctoral research at the fundamental research laboratory of NEC Corporation in Tsukuba (Japan), working with Dr. Sumio Iijima who is credited with the discovery of carbon nanotubes. Prof. Ajayan was involved in some of the seminal works on nanotubes and has continued his work in this field ever since. After NEC, he spent two years at the universite Paris-sud (Orsay) and a year and half at the Max-Planck-Institut für Metallforschung at Stuttgart as an Alexander von Humboldt fellow. Currently he is Assistant Professor at the Department of Materials Science and Engineering at Rensselaer Polytechnic Institute, Troy, New York. His main research interest concerns structure–property correlation in nanostructures and nanocomposite systems.

To form curved structures (such as the fullerenes) from a planar fragment of hexagonal graphite lattice, certain topological defects have to be included in the structure. To produce a convex structure, positive curvature has to be introduced into the planar hexagonal graphite lattice. This is done by creating pentagons. It is a curious consequence of the Euler's principle that one needs exactly 12 pentagons to provide the topological curvature necessary to completely close the hexagonal lattice; hence, in C_{60} and all the other fullerenes (C_{2n} has $(n-10)$ hexagons) there are many hexagons but only 12 pentagons. The rule of pentagon numbers will hold, however big the closed structure may be created out of hexagons and pentagons. One can thus imagine that a greatly elongated fullerene can be produced with exactly 12 pentagons and millions of hexagons.[4] This would correspond to a carbon nanotube,[1,4–8] as the geometry of the structure in Figure 1A reflects: a long cylinder made of the hexagonal honeycomb lattice of carbon, bound by two pieces of fullerenes at the ends (Figure 1B). The diameter of the tube will depend on the size of the semi-fullerene that the end is made of (e.g., a nanotube based on C_{240} as in Figure 1B will have a diameter of around 1.2 nm).

10.1021/cr970102g CCC: $35.00
Published on Web 05/01/1999

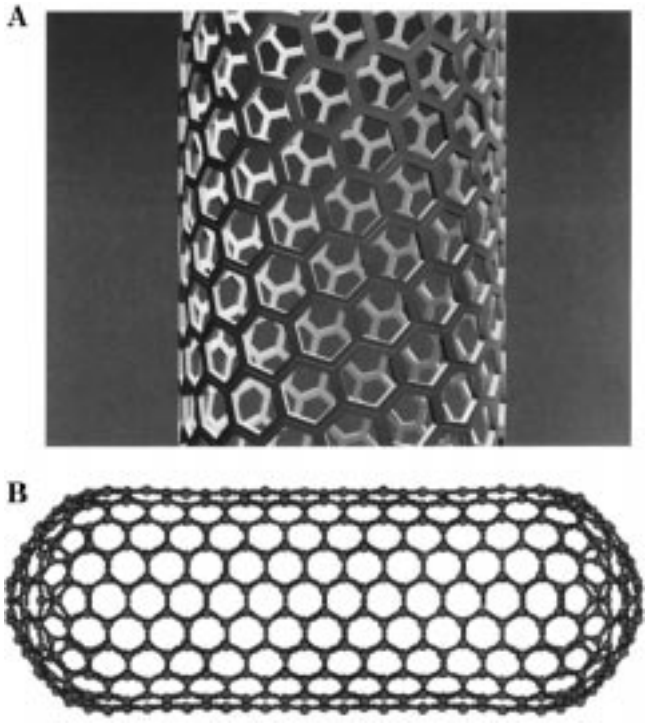

Figure 1. (A) Schematic of the basic unit of a carbon nanotube. The cylindrical structure is built from hexagonal honeycomb lattice of sp^2 bonded carbon with no dangling bonds. (Reprinted with permission from ref 6. Copyright 1997 Institute of Physics.) (B) Shows the schematic of a closed fullerene tubule (Courtesy, Dr. J.-C. Charlier). Note that in panel A the lattice is wound helically around the tube axis but in panel B there is no helicity. The ends of the tubule in panel B are made of hemispherical domes that are pieces of a fullerene.

One could start with a sheet of graphene (single layer of graphite) and fold it into a cylinder such that the open edges match perfectly to form a seamless structure. This operation will result in an open ended tube. The tubes have to be closed at both ends, which means that at some stage in the growth process pentagons are nucleated to initiate the closure mechanism. The rolling up of graphene sheets into cylinders does not describe the structural subtlety of nanotubes completely. The rolling can be done in several ways, still satisfying the criterion that the dangling bonds present at both edges are matched. Any translational shift along the edges before fitting the dangling bonds will lead to a different orientation of the lattice with respect to an arbitrary tube axis. Thus, in a general nanotube structure, on the curved surface of the tube the hexagonal arrays of carbon atoms wind around in a helical fashion, introducing *helicity* to the structure.

In the mapping of a graphene plane into a cylinder, the boundary conditions around the cylinder can be satisfied only if one of the Bravais lattice vectors (defined in terms of the two primitive lattice vectors and a pair of integer indices (n_1, n_2)) of the graphene sheet maps to a whole circumference of the cylinder[9,10] (Figure 2). This scheme is very important in characterizing the properties of individual nanotubes as they provide the essential symmetry to the nanotube structure. Nanotubes made from lattice translational indices of the form (n, 0) or (n, n) will have two helical symmetry operations where as all other

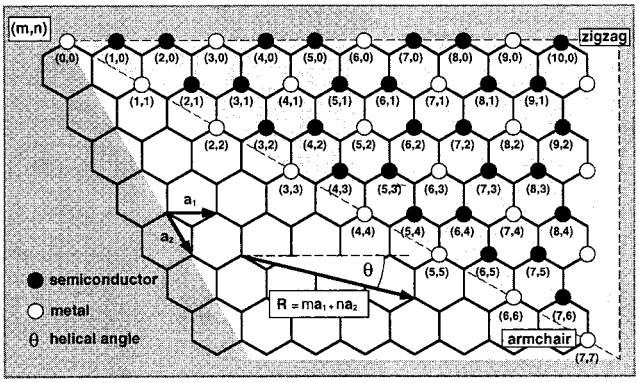

Figure 2. Indexing scheme that shows the folding procedure to create nanotube cylinders from planar graphene sheets. $\mathbf{a}_1$ and $\mathbf{a}_2$ are the primitive lattice vectors of the hexagonal lattice. The position and length of the vector, **R**, connecting an origin to the lattice point that defines the nanotube index, determine the helicity and diameter of the tube. All the (n, n) type nanotubes form armchair tubes and all (n, 0) tubes are zigzag tubes. (Reprinted with permission from ref 6. Copyright 1997 Institute of Physics.)

sets of nanotubes will have the three equivalent helical operations. The (n, 0) type of nanotubes are in general called zigzag nanotubes where as the (n, n) types are called armchair nanotubes; all others will be helical.

The helicity in nanotubes was the most revealing discovery that emerged out of the first papers by Iijima.[11,12] Electron diffraction taken from individual nanotubes showed that the orientation of the top and bottom portions of the individual nanotube cylinders (with respect to the tube axis) can be different, indicating helicity in the lattice. Recently, clear images (by scanning tunneling microscopy, STM) of atomically resolved structures of the nanotube surfaces have verified the helical structure.[13−15] This subtle variation in the structure has great relevance since early theoretical modeling showed that nanotube properties change as a function of helicity and tube diameter.

Nanotubes form in two categories. The first, called the multiwalled carbon nanotubes (MWNT) were the first to be discovered. These are close to hollow graphite fibers,[16] except that these have a much higher degree of structural perfection. They are made of concentric cylinders placed around a common central hollow, with a spacing between the layers close to that of the interlayer distance in graphite (0.34 nm) (Figure 3A). This interlayer spacing in MWNT is slightly larger than the single-crystal graphite value (0.335 nm) since in these tubes there is a severe geometrical constraint when forming the concentric seamless cylinders while maintaining the graphite spacing between them. The three-dimensional structural correlation that prevails in single-crystal graphite (ABAB stacking) is lost in the nanotubes, and the layers are rotationally disordered with respect to each other. The second variety is close to an ideal fullerene fiber; in size they are close to fullerenes and have single-layer cylinders extending from end to end.[12,17] These are called the single-walled nanotubes (SWNT) and possess good uniformity in diameter (1−2 nm) (Figure 3B). When produced in the vapor phase, the SWNT self-as-

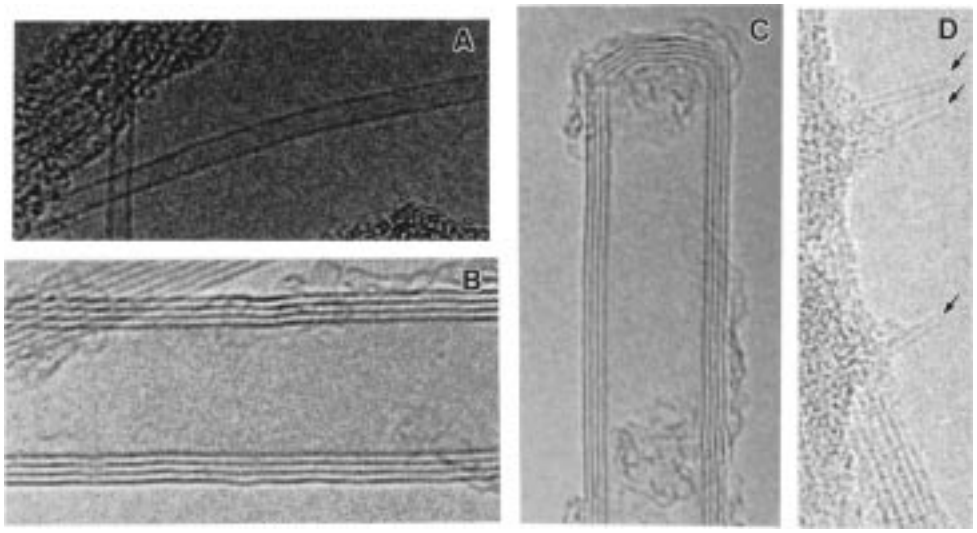

Figure 3. High-resolution transmission electron microscopy images of typical SWNT (A) and MWNT (B). Closed nanotube tips are also shown in panel C (MWNT tips) and panel D (SWNT tip, shown by arrows). The inner space corresponds to the diameter of the inner hollow in the tube. The separation between the closely spaced fringes in the MWNT (B, C) is 0.34 nm, close to the spacing between graphite planes. The diameter of the SWNT (A, D) is ~1.2 nm. Every layer in the image (fringe) corresponds to the edges of each cylinder in the nanotube assembly.

semble into larger bundles (ropes) that consist of several tens of nanotubes.[5,18,19] The tubes assemble into a one-dimensional triangular lattice structure with a lattice constant of 1.7 nm and tube−tube separation of 0.315 nm.[19] This organization of nanotube units into a crystal structure was predicted earlier by theory.[20] Both varieties of nanotubes can be regarded as aggregates of nanotube units (cylinders), the MWNT consisting of concentric assembly and SWNT ropes of close packed nanotube units. The aspect ratios of both MWNT and SWNT are large since their lengths are in the range of several micrometers. MWNT form in a range of diameters, typically from 2 to 25 nm.

The structure of nanotubes remains distinct from all previously known carbon fibers and filaments. Most importantly, nanotubes for the first time represent a carbon fiber, the structure of which is entirely known, to the atomic level. Carbon fibers made using traditional methods of extrusion from polymer slurries and from catalytic chemical vapor deposition vary in morphology and structure from fiber to fiber and from area to area on each fiber. Nanotubes can be regarded as a true macromolecular system with a known architecture—that of ideal graphene sheets. They can be considered as whiskers constructed from ideal in-plane graphite architecture. Since the atomic positions in the structure are known precisely, theoretical modeling can be used to predict the properties of nanotubes. It is this predictability that mainly distinguishes nanotubes from other carbon fibers and associates them with molecular fullerene species.

After the discovery of nanotubes, initial efforts were mainly geared toward characterizing these structures. Although several methods were used to obtain structural information from nanotubes, microscopy and local spectroscopy techniques have dominated the field since the spatial resolution obtainable through these techniques is compatible with the dimensions of nanotubes. Both transmission electron microscopy (TEM) and scanning tunneling microscopy/spectroscopy (STM/STS) have provided simultaneous information of the atomic and electronic structure of nanotubes, thereby verifying that the electronic properties of nanotubes depend on the diameter and helicity. The most conclusive evidence has been recent STM/STS studies which have shown atomically resolved lattices of nanotubes (Figure 4)

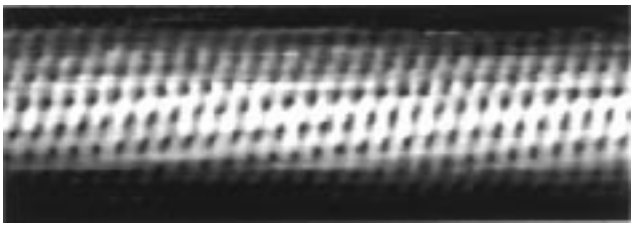

Figure 4. High-resolution scanning tunneling microscopy (STM) image showing the lattice structure of a helical semiconducting SWNT. The helical lattice is clearly revealed (Courtesy, Dr. C. Dekker). The figure is reproduced with permission from Wildöer, J. W. G.; et al. *Nature* **1998**, *391*, 59. Copyright 1998 Macmillan Magazines Ltd.

and the corresponding electronic structure of both metallic and semiconducting tubes.[14,15] In addition, and in contrast to graphite, well-spaced and symmetric structures called Van Hove singularities appear in the local density of states of nanotubes due to the one-dimensional nature of the conduction electron states in nanotubes.

Calculations have predicted that all the armchair tubes are metallic whereas the zigzag and helical tubes are either metallic or semiconducting.[1,7−8] The electronic conduction process in nanotubes is unique since in the radial direction the electrons are confined in the singular plane of the graphene sheet. The conduction occurs in the armchair (metallic) tubes through gapless modes as the valence and conduction bands always cross each other at the Fermi energy. In most helical tubes, which contain large numbers of atoms in their unit cell, the one-dimensional band

structure shows an opening of the gap at the Fermi energy, and this leads to semiconducting properties. This unique electronic behavior only occurs for small nanotubes. As the diameter of the tubes increases, the band gap (which varies inversely with the tube diameter) tends to zero, yielding a zero-gap semiconductor electronically equivalent to the planar graphene sheet. In a MWNT, the electronic structure of the smallest inner tubes are superimposed by the outer, larger planar graphene-like tubes. This has been substantiated by experiments[21,22] where the band structure obtained from individual MWNT resembles that of graphite. Experiments have indicated that the pentagonal defects present at the tips can induce metallic character by introducing sharp resonances in the local density of states near the Fermi energy.[22] Similar metallization of the nanotubes is also found to occur through substitutional doping of the nanotube lattice with impurities such as boron and nitrogen.[23]

The vibrational modes (phonons) in carbon nanotubes are extremely interesting since the spectrum varies as a function of nanotube diameter, due to changes of the unit cell and the number of atoms in the unit cell with size. Some of the vibrational modes in nanotubes (as in graphite) can be excited by Raman spectroscopy (Figure 5). Using the right

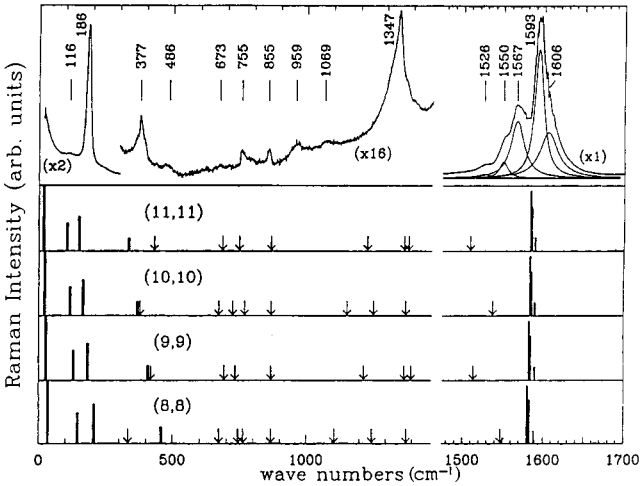

Figure 5. Experimental Raman spectra (using 514.5 nm wavelength laser probe) from nearly pure SWNT samples showing several peaks, some of which are structure sensitive and some structure insensitive (Courtesy, Dr. P. Eklund). The four bottom panels are calculations of Raman modes from nanotubes of helicity shown in brackets. Arrows show positions of weak Raman peaks. The figure is reproduced with permission from Rao, A. M.; et al. *Science* **1997**, *275*, 187. Copyright 1997 American Association for the Advancement of Science.

energy (frequency) of the Raman probe (laser light), phonons can be excited in SWNT of specific diameters.[24] The position of breathing modes in the Raman spectra shifts with the diameter of the tubes, and this can be used to determine which diameter is in resonance with the laser frequency. Such resonant Raman scattering has become a powerful tool in mapping the distribution of nanotube diameters in bulk samples,[25,26] a task that is almost impossible with local imaging techniques.

II. Assembly in Carbon Soot

In his first experimental report, Iijima showed MWNT sticking to the ends of graphite electrodes that were used in the production of fullerenes. Fullerenes are formed in vapor, in the carbon soot formed by the evaporation of graphite electrodes. MWNT are formed on the cathode surfaces used in such soot generation. A year after the discovery of MWNT, it was found that if conditions are right the evaporated carbon can be directed to condense continuously on the cathode surface into a cigar-like deposit, which builds up into a few centimeter long boule made of a graphite shell packed with nanotubes and closed graphite nanoparticles.[27] The technique is similar to what Roger Bacon had used almost three decades ago[28] to generate large (micrometer size) arc-grown carbon whiskers, although he used very different conditions in his experiment. The method also derives from the Kratschmer−Huffman method of generating fullerenes.[29] To generate MWNT, a dc arc is usually used (with a modest voltage of 20 V and currents of <100 A) in an inert atmosphere of 500 Torr of helium. It is quite amazing that such highly ordered nanotubular structures self-assemble in the plasma created in the interelectrode region, where temperature is close to 3500 °C. The time scale of formation of these nanostructures is extremely small; a 5 nm MWNT of 1000 μm length grows in 10^{-4} s.[30]

The inside of the deposit formed in the electric arc discharge contains a highly porous network of randomly oriented MWNT structures (Figure 6) which

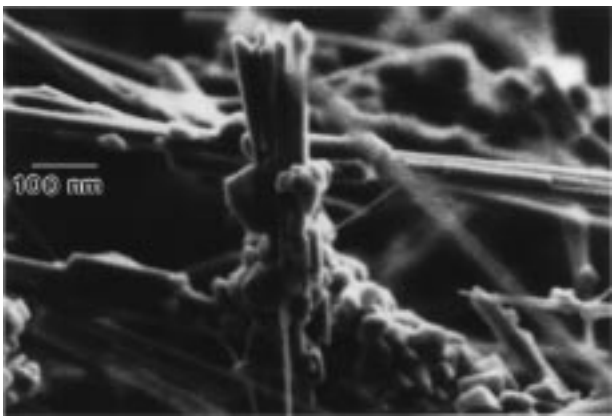

Figure 6. SEM image of multiwalled nanotubes grown in the electric arc. Both nanotubes and polyhedral nanoparticles are seen.

are organized on a macroscopic scale into pencil-like columns aligned in the axial direction of the deposit. The electric arc method produces the stiff, near-perfect, and whiskerlike MWNT (suggesting superior properties compared to catalytically grown[16] carbon nanofibers) although some reports suggest that the high temperature of the arc could produce sintering and cross-linking between tubes.[31] However, the arc technique suffers from drawbacks. Being a batch process, the amount of material that can be produced is limited and the material that is formed in the deposit contains substantial amounts of nanoparticles which have polyhedral shapes and are low in aspect ratio. There have been several attempts, in

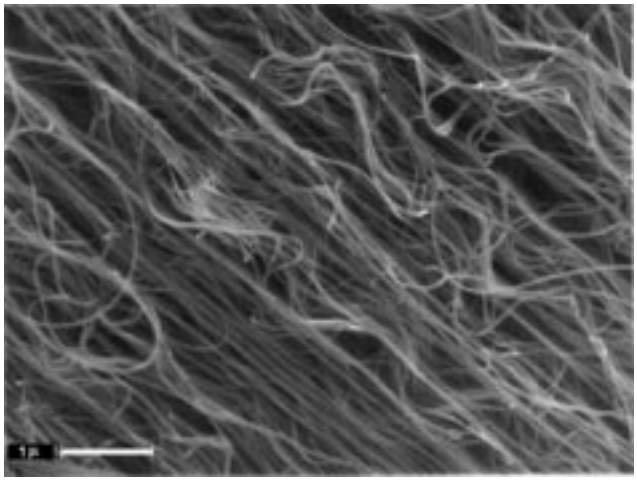

Figure 7. SEM image showing multiwalled carbon nanofibers made by pyrolisis of triazine precursors on laser etched Co catalyst particle arrays. Notice the uniformity in diameter of the fibers and good alignment between the fibers (Courtesy, Dr. M. Terrones). The figure is reproduced with permission from Terrones, M.; et al. *Nature* **1997**, *388*, 52. Copyright 1997 Macmillan Magazines Ltd.

parallel, to make nanotubes through catalytic vapor deposition, which overcomes some of the problems of the arc process. In general, catalytic metal particles are exposed to a medium containing hydrocarbon gaseous species, and the formation of nanofibrils (twisted hollow fibers) is catalyzed.[32,33] One good example is the Hyperion fibers, which have been in commercial use[33] for at least a few years. During growth, good uniformity in size of the fibers is achieved (controlled by the size of the seeded catalyst particles), and the process can be easily scaled up to produce large amounts of material. In some cases, when the catalysts are prefabricated into patterned arrays, well-aligned nanotube assemblies are produced (Figure 7).[34,35] Similarly, template based approaches are also in use, where the aligned pores of a nanoporous membrane (such as electrodeposited porous alumina) are filled with carbon species through vapor deposition and later graphitized to produce nanotubes and then the template membrane is removed to obtain aligned, nanotube arrays.[36] Another approach that has been recently successfully demonstrated is the use of plasma-assisted hot filament chemical vapor deposition[37] in conjunction with plasma-assisted modification of the catalyst surface (such as Ni deposited on Si). Large scale arrays of vertically aligned (to the substrate) nanotubes have been fabricated by this method.

Single-walled nanotubes are made using a combination of catalyst and dense carbon vapor. Both are simultaneously introduced into an inert atmosphere by either an electric arc[17,19] or through laser ablation.[18] In the former, the setup is similar to that used for MWNT synthesis, but a hole is drilled in the anode and packed with a mixture of the metal catalyst and graphite powder. Several metals and combinations of metals have been tried to obtain good yield of nanotubes, and the best so far is for a mixture of Ni and Y with graphite in a 15:5:80 weight ratio. When the electric arc is struck with such a modified electrode, spectacular growth occurs in the reaction vessel which gets decorated with a network of web-like growth that contain SWNT. On a closer look the webs contain ropes of nanotubes that consist of tens of SWNT (Figure 8). The maximum density of nanotubes is seen in the growth product that forms around the cathode like a collar, and this material consists of >50 wt % nanotubes. The rest of the carbon soot contains fullerenes, partially graphitized carbon (glassy carbon), amorphous carbon, and finely distributed catalyst particles. In the laser ablation technique,[18,43] a metal (Ni−Co) containing (small percentage, <1 wt %) graphite target placed in an oven is ablated with a strong laser pulse under inert atmosphere. A felt of nanotube material that is generated is collected onto a water-cooled target using forced gas flow. The use of two coordinated laser pulses breaks down the carbon formation better, producing a very high yield of nanotubes (∼60−80%). Chemical vapor deposition (CVD) methods have been also tried for growing SWNT. Disproportionation of CO over size-selected Mo catalysts was shown[38] to produce fibrillar structures made of single graphene walls. More recently, there has been a growing interest in exploring the possibility of tailoring catalyst surfaces using conventional thin-film techniques (sputter deposition, selective etching) and then using these substrates to grow nanotubes. Kong et al.[39] have shown that catalyst islands fabricated

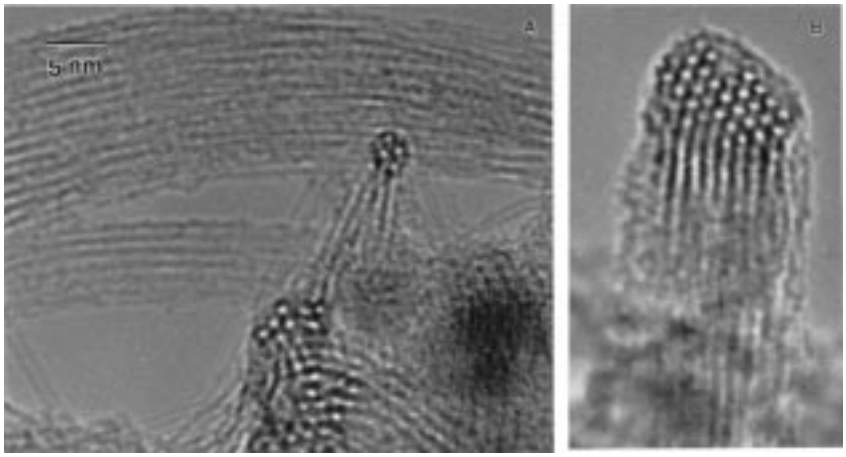

Figure 8. (A) HRTEM image of ropes of SWNT produced in the arc using Ni−Y catalyst. (B) Cross-sectional view of a SWNT rope that shows the crystal lattice of the organized nanotubes.

on Si wafers using electron beam lithography can be used to grow (by CVD) SWNT oriented in the plane of the substrate.

It is clear that the nanotube containing raw material (prepared by the electric arc or laser ablation) is not useful for any bulk measurements, since the impurity content is high. The same is true for fullerene soot. Fullerenes which form at very low yield in the soot are purified by dissolution in organic solvents followed by liquid chromatography. The problem with nanotubes is that they are insoluble in most solvents, and hence all the purification procedures follow filtration-based techniques. This means that the purified nanotube products are never as pure as fullerenes. All purification procedures follow certain essential steps; preliminary filtration to get rid of large graphite particles, dissolution to remove fullerenes (in organic solvents) and catalyst particles (in concentrated acids), and microfiltration and chromatography to either size separate MWNT and nanoparticles or SWNT and the amorphous carbon impurities.[40−43] It is important to keep the nanotubes separate when suspended in solution, and nanotubes are typically dispersed using a surfactant (e.g., sodium dodecyl sulfate) prior to the last stage in separation. Some reports claim that SWNT samples with >99% purity can be made by repeated use of some of these steps.[43] Separation of MWNT from nanoparticles is much less efficient. Initially, oxidation was used to remove nanoparticles from MWNT samples (Figure 9)[44,45] but some of the nanotubes in

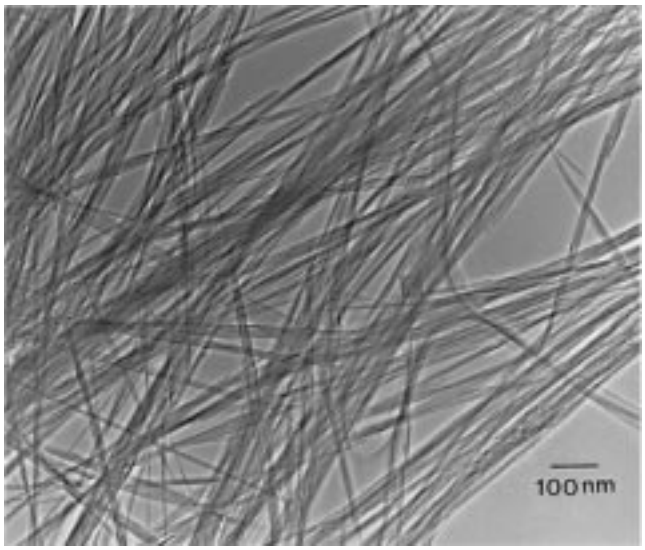

Figure 9. TEM image of purified MWNT sample. Most of the polyhedral nanoparticles have been removed by oxidation in air at 750 °C. The nanotubes in such oxidized samples are all open.

the sample also gets destroyed in the process. Recent efforts[40] to use size exclusion chromatography and cascade filtration have yielded good separation between nanotubes and nanoparticles in the samples. But these methods are impossible to scale up to obtain larger volumes of samples.

It is now possible to cut nanotubes (SWNT) into smaller segments by extended sonication (agitation using ultrasound) in concentrated acid mixtures.[43] The idea of cutting nanotubes by ultrasound was first demonstrated for MWNT.[46] The resulting pieces of broken SWNT (open pipes that are typically a few hundred nanometers in length) form a colloid suspension in solvents which can be deposited on substrates or further manipulated in solution and functionalized at the ends. Such segments can perhaps be joined using the right chemical bridges to make long nanotube chains resembling polymers. A whole gamut of possible chemistry based on nanotubes is just beginning to unfold. It has been recently shown[47] that functionalized nanotubes (derivatized with thionychloride and octadecylamine) can be dissolved in organic solvents. Extensions of this technique may in the future be used to separate nanotubes using solvation and produce high-purity, well-defined samples.

Since size and helicity are two important parameters that affect nanotube properties, selection on the basis of both these factors is important. This is mostly relevant to SWNT, since the MWNT only show average properties and tend to be semimetallic as parent graphite. Fortunately the size distribution produced during the high-yield synthesis of SWNT is quite narrow with an overwhelming majority of the nanotubes having diameters close to 1.4 nm. It has been shown[25,5] that it is possible to tune nanotube diameter in the range between 1.2 and 6 nm by altering the temperature (from 700 to 1200 °C) of the ambient in which these are formed or by the addition of impurities such as Bi and S to the transition metal catalysts. It is fortuitous[18] that when SWNT are formed in high yield, a vast portion of the tubes have armchair (or close to armchair) arrangement independent of the conditions used in the synthesis. This size and helicity selection will have a strong bearing on the possible usability of nanotubes, especially in electronics.

It should be stated that there is no consensus yet on the mechanism by which nanotubes grow. One problem is that the experimental conditions in which nanotubes grow are too chaotic to deduce any meaningful relationship with growth models. Hence most of the explanations for nanotube growth have been based on theoretical modeling of the energetics[48] and molecular dynamics simulations which consider only a small number of atoms.[49,50] One distinction between the two varieties of nanotubes is that the MWNT grow with no catalysts whereas SWNT grow only when catalysts are present. But unlike larger catalytically grown fibers, where the fiber ends are seen decorated with catalyst particles, the ends of SWNT are always closed with no trace of catalyst. One could imagine that SWNT grow with the aid of catalyst species at the end but are somehow ejected as the tube closes into the fullerene caps. Assuming that the tubes remain open, a suggestion was that catalyst atoms are attached to the dangling bonds of the tube ends and promote growth by a scooter mechanism, acting as a dynamic bridge, incorporating incoming carbon atoms to the open ends of tubes.[18] But simulations have shown that this is far from the truth since the metal atom decorated tubes tend to close instantaneously at close to growth tempera-

tures, ejecting the metal atoms from their edges.[49] A simple chemical explanation has also been put forward[51] to explain the preferential formation of SWNT of the observed sizes. On the basis of strain and reactivity, it is seen that C_{240} is the most chemically inert fullerene, suggesting these may act as precursors for the preferential nucleation of (10, 10) nanotubes which are ~1.4 nm in diameter. For MWNT, it is a different story; it is seen during simulations that chemical bonding between the open edges of adjacent coaxial tubes (called a lip−lip interaction) can stabilize the open ended growing structures.[42,43] This welded end geometry of tubes shows high chemical activity and easily incorporates incoming atoms for growth. Understanding the growth mechanisms of nanotubes still remains a big challenge.

III. Distinguishing Properties

What makes nanotubes so special is the combination of dimension, structure, and topology that translates into a whole range of superior properties. The basic constitution of the nanotube lattice is the C−C covalent bond (as in graphite planes) which is one of the strongest in nature. The perfect alignment of the lattice along the tube axis and the closed topology endows nanotubes with in-plane properties of graphite such as high conductivity, excellent strength and stiffness, chemical specificity, and inertness together with some unusual properties such as the electronic structure which is dependent on lattice helicity and elasticity. In addition, the nano-dimensions provide a large surface area which could be useful in mechanical and chemical applications. The surface area of MWNT has been determined by BET techniques and is ~10−20 m^2/g, which is higher than that of graphite but is small compared to activated porous carbons. This value for SWNT is expected to be an order of magnitude higher. Similarly, due to the relatively large hollow channels in the center of nanotubes, their density should be very low compared to graphite. Rough estimates suggest that SWNT density could be as small as 0.6 g/cm^3, and MWNT density could range between 1 and 2 g/cm^3 depending on the constitution of the samples.

The remarkable electronic properties of nanotubes were noted earlier. Both metallic and semiconducting SWNT have been observed through calculations and experimental verifications of their band structure (Figure 10). Simultaneous determinations of helicity by STM have proved several theoretical predictions. The most exciting and challenging have been transport measurements in individual nanotubes by four or more probe measurements. Systematic four-probe measurements on several individual MWNT showed a range of electronic behavior (metallic, semiconducting, and semimetallic) in these structures.[52−54] A weak magneto-resistance in the tubes indicates a very short mean free path for the conduction electrons, most likely due to scattering by defects. MWNT is composed of several cylinders of different helicity, and this complicates any simple interpretation of transport, based on theoretical predictions. It is, however, clear that the conduction properties in MWNT are also unique, and recent reports have

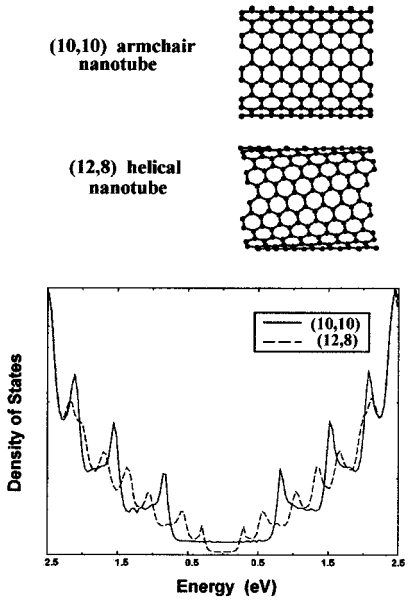

Figure 10. Electronic properties (DOS) of SWNT [(10, 10) armchair and (12, 8) helical nanotube] close to the Fermi energy. A "plateau" is clearly seen for the armchair tube (metallicity) and the small gap related to the helical one (Courtesy, Dr. J.-C. Charlier).

observed ballistic electron transport at room temperatures[55] and the Aharnov−Bohm effect[56] in individual MWNT. In contrast to MWNT, SWNT is a well-defined system in terms of electronic properties. Electron transport measurements have been possible on individual SWNT and SWNT ropes randomly dropped on prefabricated electrode assemblies.[57] Measurements carried out in the milli-Kelvin range show that conduction occurs through well-separated discrete electronic states which are coherent over distances between the probes (a few hundred nanometers). Results of these experiments prove that indeed individual SWNT can be regarded as quantum wires. Calculations show that, unlike normal metal wires, conduction electrons in (armchair) SWNT experience an effective disorder averaged over the tube's circumference, leading to electron mean free paths that increase with nanotube diameter. This increase could result in exceptional ballistic transport properties and localization lengths of several micrometers.[58] Recent experiments provide evidence to the uniqueness of the electron system in SWNT ropes,[59] where the measurements of conductance as a function of temperature and voltage agree with predictions for tunneling into a Luttinger liquid (strongly correlated one-dimensional electron systems).

The electrical conductivity of nanotubes can be altered by modifying the parent structure of the nanotube lattice. In MWNT, substitutional doping can be done to the lattice of nanotubes. The addition of boron and nitrogen in these structures has been shown to create metallic features in the electronic density of states.[23] SWNT ropes have been doped with alkali and halogen dopants which act as intercalates that go into the interstices between the tubes in ropes, and the charge transfer between the tubes and the dopants produce an order of magnitude increase in the electrical conductivity.[60,61] The doped

nanotubes may be considered to be a new generation of unique synthetic metals.

Apart from their electronic properties (a detailed review of nanotube electronics is scheduled to appear in a future issue of this journal), the mechanical properties of nanotubes are equally fascinating. The strength of the carbon bonds makes nanotubes one of the strongest and stiffest materials known. On the basis of the in-plane elastic modulus of graphite, the axial elastic modulus of nanotubes is predicted to be at least one TPa (1000 GPa).[62,63] Experiments to measure the elastic properties of individual nanotubes were initially considered impossible. Some clever recent experiments including new techniques using scanning probe microscopes have helped in estimating the local elastic properties of materials and have provided valuable answers to the question of nanotube strength. In one experiment, the estimates of the elastic modulus and stiffness of nanotubes were obtained from measuring their thermal vibrational amplitudes.[64] Nanotubes projecting out into the holes of a sample holder (used in electron microscopy measurements) were considered as cantilevers clamped to a support, vibrating with their natural thermal vibration frequencies. The average value for the modulus of MWNT obtained (1.8 TPa) by this method was higher than that of the in-plane value of graphite. Atomic force microscopy measurements of nanotube response during bending and manipulation[65,66] provide values of the elastic modulus close to the 1 TPa range. From all the measurements and theoretical work to date, it can be said that the elastic modulus of nanotubes and the corresponding stiffness of nanotubes are similar to (and perhaps greater than, due to the new topology) the in-plane values of the parent graphite sheet. Atomic force microscopy experiments have probed[67] the motion of nanotubes on substrates such as graphite. These experiments have revealed fascinating characteristics of nanotube friction, suggesting that depending on the orientation of the nanotube on the substrate various forms of lock-in movements can occur, for example, a transition from rolling to sliding of the tubes.

The hollow structure and closed topology of nanotubes produce a distinct mechanical response in nanotubes compared to other graphitic structures. The fracture and deformation modes of nanotubes are intriguing. Nanotubes can sustain extreme strains (40%) in tension without showing signs of brittle behavior, plastic deformation, or bond rupture.[7] Fracture can occur in a nanotube via the collapse of the inside hollow providing extra absorption of energy and increased toughness when used in composites.[68] Fracture of individual nanotubes under tensile loading has been evidenced in molecular dynamics simulations.[69] Elastic stretching elongates the hexagons on the tube surface until at high strain some bonds are broken. This local defect is easily redistributed over the entire surface due to the mobility of these defects in the two-dimensional lattice. A new form of necking slowly sets in until the tube is locally reduced to a linear chain of carbynes (carbon atoms linked by double bonds into a chain). Nanotube plasticity manifests itself in other curious ways too. It has been suggested that a 5−7 ring pair defect, called a Stone−Wales defect[70] in sp^2 carbon systems, in the nanotube lattice can become mobile under the influence of stress. This leads to a stepwise size reduction of the nanotube diameter.[71] The process introduces a change in helicity in the deformed nanotube structure. This extraordinary behavior could lead to another application; a nanotube probe (sensor) that responds to mechanical stress by changing its electronic character.

The topology leads to stepwise deformation behavior in nanotubes. Highly deformed nanotubes were seen (in simulations) to reversibly switch into different morphological patterns with abrupt release of energy[63] (Figure 11). The patterns are interesting in

Figure 11. Simulations showing two possible ways nanotubes can deform when they are loaded. The modes reflect the highly elastic nature of nanotubes (Courtesy, Dr. B. I. Yakabson). Details of the deformation mechanisms are reported in Yakabson, B. I.; Brabec, C. J.; Bernholc, J. *Phys. Rev. Lett.* **1996**, *76*, 2511.

all forms of deformation, for example, in torsion the nanotubes first flatten and then get twisted in a loop. The reversibility of deformations such as buckling has been seen in TEM studies (Figure 12) and supports the idea that nanotubes are highly elastic. This behavior is related to the in-plane flexibility of the graphene sheet and the ability for carbon atoms to rehybridize with the degree of sp^2-sp^3 rehybridization depending on the strain.

Carbon materials and graphite fibers have been used in industry to improve thermal conduction. The in-plane thermal conductivity of graphite (∼3000 W/m K) is second only to certain forms of doped diamond. Since nanotubes reflect the in-plane properties of graphite, their thermal conductivity should also be extremely high. High aspect ratios also improve drastically the thermal conductivity of discontinuous fiber composites. No one has reported any thermal measurements on nanotubes yet, but nano-

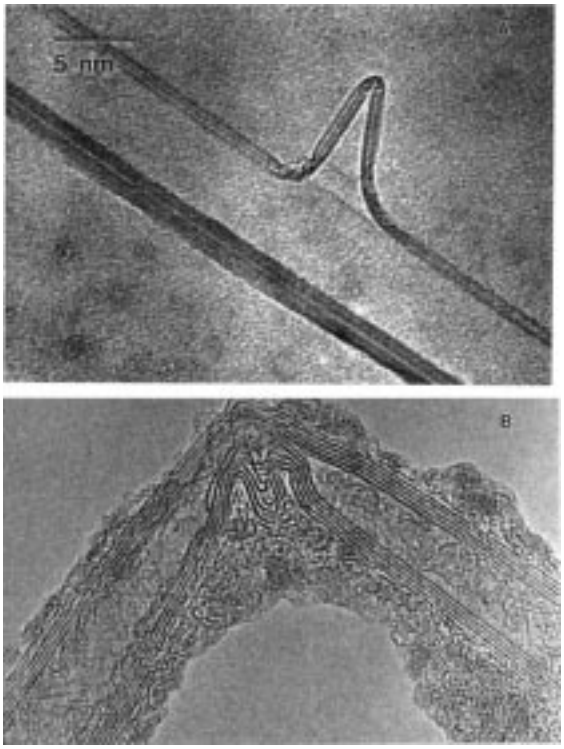

Figure 12. (A) TEM image of a buckled MWNT (in a polymer film) due to compressive stress produced during cutting of the film. This buckling behavior in nanotubes is observed to be reversible for free-standing nanotubes once the load is released. Notice the adjacent larger nanotube has not buckled, suggesting that it depends on nanotube size and wall thickness. (B) HRTEM showing the deformation of individual layers during the buckling of an individual MWNT. Spacing between the parallel fringes (layers) on the tube (B) corresponds to 0.34 nm.

tubes could be an ideal filler material that could improve conductivity, especially in composites. The thermal expansion coefficient of nanotubes will also be unique compared to graphite. Graphite is highly anisotropic with negligible thermal expansion in-plane but significant out-of-plane expansion. Nanotubes, on the other hand, are constrained by geometry and should have nearly zero expansion normal to the planes.

Initially, it may seem that nanotubes are chemically inert since the only exposed surface in nanotubes is the unreactive basal graphite plane. Oxidation studies show that the ends of nanotubes are more reactive than the cylindrical parts.[72,73] When the tubes are oxidized the tube ends get etched away, resulting in open tubes. The presence of pentagonal defects at the ends and the extra dimensional curvature (and strain) caused by these defects are responsible for this enhanced tip reactivity. Recent experiments suggest that nanotube surfaces show enhanced electron transfer rates when used as electrodes in chemical reactions.[74] The role of MWNT in the electrocatalysis of oxygen reduction has been demonstrated, and charge transfer on nanotubes is seen to occur faster compared to graphite. Ab initio calculations performed on SWNT show that curvature of the tubes leads to only a slightly larger charge transfer that tends as $1/D$ (D is tube diameter) to graphitic values (2% larger for a nanotube with $D =$ 0.82 nm). This slight increase is attributed to curvature induced $\sigma-\pi$ hybridization that alters the energy band dispersion close to the Fermi energy. However, the average Mulliken population (charge density) at a pentagon is 3−4 times larger than at a graphene hexagon in both planar and tubular structures. It is thus clearly seen that due to the higher density of states at the pentagonal sites these would act as electrophilic reaction sites (Figure 13). In

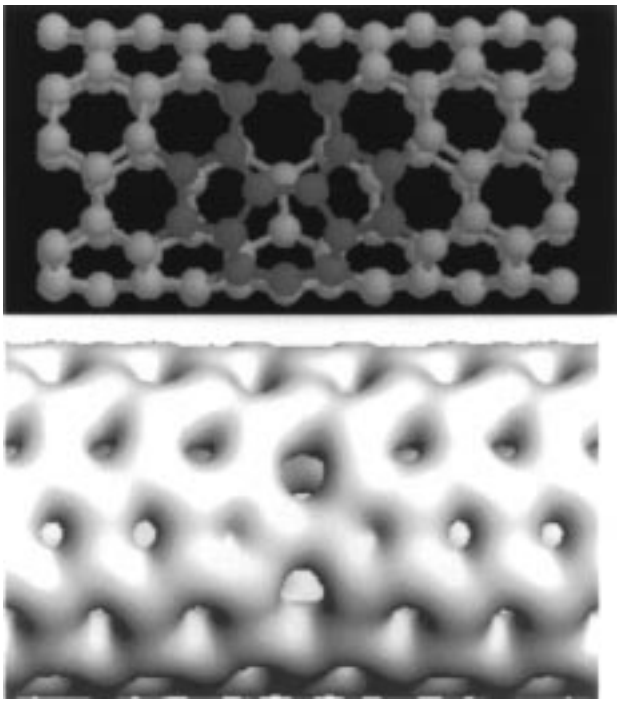

Figure 13. Top: ball-and-stick model for a single-walled nanotube (6, 6) with a bond rotation defect (two 5−7 pairs) (gray atoms in the structure). Bottom: corresponding simulated 3D-local density of states image (similar to what is observed in an STM) of occupied orbitals around the Fermi level for this tube. An increase in the available density of states at the pentagonal sites is seen with respect to hexagonal or heptagonal sites.

nanotubes, the presence of large numbers of topological defects (e.g., bond rotational defects or pairs of 5−7 rings; defects which would not create any visible change in the overall topology or curvature) has been suggested[4] and hence the surface of nanotubes could be inherently more reactive compared to their graphite counterparts.

Finally, nanotubes have one distinguishable feature which is the smooth, straight, one-dimensional channel in their centers. Early calculations showed that since capillarity force could be strong in these structures (dimensional effect),[75] the inside channels could hold atoms or molecules of other species. It has been experimentally demonstrated that nanowires can be created inside nanotubes,[76−78] as detailed in a separate paper soon to appear in this journal. This brings about the unique possibility of using nanotubes as nanosize container systems or as unique templates for fabrication of novel nanomaterials.

IV. Nanotubes for the Marketplace

It seems reasonable to think that with all the exciting properties mentioned above, carbon nano-

tubes will find commercial applications. Several experimental demonstrations have already pointed to possible uses for this material. It is conceivable that nanotubes will be important players in future technology, especially as part of the ongoing revolution based on nanotechnology and nanostructures which is the theme of this journal issue.

The remarkable electronic properties of nanotubes qualify them for use as quantum wires and in heterojunction devices. The Delft group, which pioneered the measurements of electron transport in individual SWNT, has built the first single-molecule field-effect transistor based on a single semiconducting SWNT.[79] The device, which operates at room temperature, is comprised of a nanotube bridging two metal electrodes. The band structure suggested for this device is similar to traditional semiconductor devices, and the performance of this device is comparable to existing devices in terms of switching speeds. Although the demonstration of such a device is exciting, the next stage of integrating devices into circuits will be crucial. None of the procedures developed so far for nanotube fabrication enables the construction of complex architectures that the semiconductor industry requires today. New ideas based on self-assembly of carbon structures into integrated nanotube assemblies will have to be realized before nanotube electronics become a practical reality. The possibility of connecting nanotubes of different helicity through the incorporation of 5−7 defect pairs could lead to the fabrication of heterojunction devices, as predicted by theory.[80] Similarly, a junction device can be designed from two nanotube segments, one of which is semiconducting and the other made metallic by doping with substitutional impurities, as in traditional semiconductors. The foundations for a whole range of physics at the nanoscale based on nanotube structures have already been laid through theoretical models, predictions, and a few recent experiments.

The second major application will be based on nanotube strength and elasticity. The most obvious one is filler-based applications in polymer composites, where traditional carbon fibers have done well. One of the main requirements for the efficient load transfer in carbon fiber (or nanotube) reinforced composites is that the interface between the fiber and the matrix be strong. There is no guarantee that one could form a strong interface in the case of nanotubes. Some recent studies have indicated that strong interfaces can be formed between epoxy resins and nanotubes (interface strengths of few hundred megapascal were observed).[81] However, these results are preliminary. The biggest advantage of nanotubes in polymer composites will be in processing, since they do not break down during processing as carbon fibers do so easily. However there are other processing problems; work done in our laboratory indicates severe settling of nanotubes in epoxy-based composites during processing. There are other fundamental questions associated with the effectiveness of nanotube reinforcements. Nanotubes remain twisted and curved when processed to make polymer composites (Figure 14), and the advantage of high aspect ratio may not be realized in nanotubes because of this

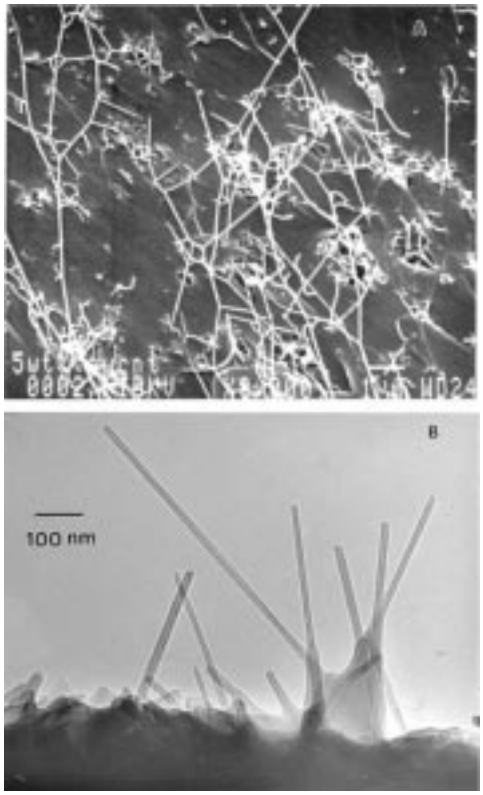

Figure 14. (A) SEM image of a typical fracture surface in a SWNT-epoxy resin composite. Notice the curved network of the nanotube ropes in the composite. (B) Projection of MWNT at the broken surface of a nanotube-PPV composite. Notice a thin layer of polymer web that joins the nanotubes together.

highly elastic behavior. It is likely that individual nanotube layers may slide with respect to each other in nanotube aggregates during stress transfer since the intertubular bonding is always weak in MWNT and SWNT ropes. Micro-Raman spectroscopy, which is used to measure the strain carried by MWNT during loading, has shown that the load transfer (from matrix to the nanotubes) in compression is better than in tension.[82] This suggests that under tension, only the outer layers of the nanotubes are loaded, whereas in compression load is transferred to all the layers.

Other than structural composites, some unique properties have been realized by physical doping (filling) of polymers with nanotubes. Recently, such a scheme has been demonstrated in a conjugated luminescent polymer, poly(*m*-phenylenevinylene-*co*-2,5-dioctoxy-*p*-phenylenevinylene) (PPV), filled with MWNT and SWNT.[83] Nanotube-PPV composites have shown increases in electrical conductivity compared to the pristine polymer of nearly 8 orders of magnitude, with little loss in photoluminescence/electroluminescence yield. In addition, the composite is far more robust than the pure polymer regarding mechanical strength and photobleaching (breakdown of the polymer structure due to thermal buildup). Preliminary studies indicate that the host interacts very little with the embedded nanotubes but that the nanotubes act as nanometric heat-sinks that prevent the buildup of large local thermal effects, which usually break down a conjugated polymer. Potential

exists for other new materials with nanotubes in polymer matrices, for example, materials for nonlinear optical properties, membrane technologies, electromagnetic induction shielding, and implant materials for biomedical applications.

With extremely small sizes, good conductivity, high mechanical strength, and elasticity, one area where nanotubes may ultimately become indispensable is in their use as nanoprobes. One could think of such probes being used in a variety of applications such as high-resolution imaging, nanolithography, nanoelectrodes, drug delivery, sensors, and field emitters. There have been experimental demonstrations in which an individual MWNT or SWNT is attached to the end of an AFM or STM tip for imaging[84] and lithography.[85] The advantage of the nanotube tip is its slenderness, providing the possibility to image features (such as surface cracks) that are almost impossible to probe using larger, blunter etched Si or metal tips. In addition, due to the high elasticity of nanotubes, the tips do not suffer from crashes on contact with the substrate; any impact will cause buckling in the nanotube structure which is reversible. However, the use of nanotubes as AFM−STM tips has disadvantages. The lateral resolution obtainable is low compared to STM, and it is not easy to prepare individual tips. The best use could be as AFM tips on nonperiodic structures where the resolution can be considerably improved over commercially available tips, if everything else (such as the proper anchoring of the nanotube) works well. Nanotubes functionalized at the ends with various functional groups can also be used as unique nanoprobes for performing local chemistry and biochemistry. This concept has been recently demonstrated[86] elegantly by using chemically modified nanotube tips to do nanotitration. Open ended nanotubes were functionalized by attaching carboxyl groups at the ends, and these modified nanotubes were used as AFM tips to image patterned samples based on molecular interactions and forces in biomolecular interactions.

The small dimensions of nanotubes, as well as their tip structure, make them useful as efficient field emitters. Field emission characteristics of nanotube tips have been studied, and field emission has been demonstrated from partially aligned nanotube films.[87,88] Nanotube films field emit with threshold voltages of a few tens of volts, emitting electrons at current densities of a few hundred mA/cm^2. The nanotube electron source remains stable over several hours of field emission and is air stable. One of the major problems here could be in achieving uniform emission from larger areas. The advantages of SWNT vs MWNT for field emission are being studied rigorously by several groups.

Finally, carbon nanotubes are being considered for energy production and storage. Carbon fiber electrodes have been used previously in fuel cells, battery, and several other electrochemical applications.[16,36] Nanotubes are special since they have high surface specificity and, as described before, have been shown to be superior in electron transfer reactions. Nanotube microelectrodes have been constructed using a binder and have been successfully used in bioelectrochemical reactions (e.g., oxidation of dopamine).[89] Their performance has been found to be superior to other carbon electrodes in terms of reaction rates and reversibility. Pure MWNT and MWNT deposited with metal catalysts (Pd, Pt, Ag) have been used to electrocatalyze oxygen reduction reactions which are important for fuel cells.[36] It is seen from several studies that nanotubes could be good replacements for conventional carbon-based electrodes.[74] Similarly, the improved selectivity of nanotube-based catalysts have been shown in heterogeneous catalysis. Nanotube-supported Ru particles were found to be superior to the same metal on graphite and other carbons in the liquid-phase hydrogenation reaction of cinnamaldehyde.[90] The properties of catalytically grown nanotubes have been found desirable for high-power electrochemical capacitors.[91]

Since nanotubes are excellent container systems, they could be useful material in hydrogen storage. Temperature-programmed desorption spectroscopy has shown that hydrogen will condense inside SWNT under conditions that do not induce adsorption in traditional porous carbon material.[92] It was reported that hydrogen uptake is high and can be compared to the best presently available material (metal hydrides). If an optimum diameter of the nanotube can be established for the best intake and release of hydrogen, high-energy storage efficiency can be obtained, and the process could operate at ambient temperature. Since solid fuel cells are increasingly becoming part of future technology, the role of nanotubes as energy storage materials should be significant. A statement of caution should be added here since the experiments on hydrogen storage in nanotube samples have been controversial and not reproducible on high-quality samples.

V. Conclusions

Since their discovery in 1991, nanotubes have come a long way. Several detailed reviews,[5,6] books,[4,8] and special issues of journals[93,94] have been devoted to this topic. There have been great improvements in synthesis techniques, which can now produce reasonably pure nanotubes in gram quantities. However, there is still a need to develop and optimize processing methods to make well-defined (in terms of structure and dimensions) and well-organized nanotubes, since this will have real impact on applications. For bulk applications, the quantities that can be made still fall far short of what industry would need. The market price of nanotubes is also too high presently (~$200 per gram for MWNT to 10 times that value for purified SWNT) for any realistic commercial application. But it should be remembered that the starting prices for carbon fibers and fullerenes were also prohibitively high during their initial stages of development, but their prices have come down significantly in time.

Studies of structure−topology−property relations in nanotubes have been strongly backed, and in some cases preceded, by theoretical modeling. This synergy has been of great benefit to the development of the field. Clearly, from the physics point of view, nanotubes stand out from carbon fibers since their struc-

ture is predictable. Every atom position in the nanotube (for a SWNT, which is the ideal molecular fiber) is precisely known, and the periodicity in the lattice can be reduced to a unit cell picture (as in perfect crystals), allowing its properties to be predicted. A Nanotube is the most ideal structure one could construct from the graphite architecture, and the nature (physical properties) of in-plane graphite is reflected in its properties.

The combination of the excellent properties inherited from the parent in-plane graphite and a set of unique properties due to the small dimensions, closed topology, and lattice helicity provides nanotubes with a host of properties that are remarkable. It is hard to find another material with such a range of promising properties. Some of these extraordinary properties can be utilized in the future for practical applications. Nanotubes as quantum wires in electronic devices is a promising field, but the challenges in fabrication may prohibit real device applications for several years. More imminent seem to be applications based on a combination of nanotubes and other materials, such as filled polymers. These tiny structures that self-assemble with perfection from among the mess of carbon soot could one day become indispensable nanoprobes in our daily lives.

VI. Acknowledgments

The author acknowledges support from the National Science Foundation (CAREER program) and the donors of the Petroleum Research Fund (administered by the ACS) for continuing work on carbon nanotubes.

VII. References

(1) Dresselhaus, M. S.; Dresselhaus, G.; Eklund, P. C. *Science of Fullerenes and Carbon Nanotubes*; Academic Press: New York, 1996.
(2) Rohlfing, E. A.; Cox, D. M.; Kaldor, A. *J. Chem. Phys.* **1984**, *81*, 3322.
(3) Kroto, H. W.; Heath, J. R.; O'Brien, S. C.; Curl, S. C.; Smalley, R. E. *Nature* **1985**, *318*, 162.
(4) Ebbesen, T. W. *Carbon Nanotubes: Preparation and Properties*; CRC Press: Boca Raton, FL, 1997.
(5) Kiang, C. H.; Goddard, W. A.; Beyers, R.; Bethune, D. S. *Carbon* **1995**, *33*, 903.
(6) Ajayan, P. M.; Ebbesen, T. W. *Rep. Prog. Phys.* **1997**, *60*, 1025.
(7) Yakabson, B. I.; Smalley, R. E. *Am. Sci.* **1997**, July−August, 324.
(8) Saito, R.; Dresselhaus, M. S.; Dresselhaus, G. *Physical Properties of Carbon Nanotubes*; World Scientific: New York, 1998.
(9) Mintmire, J. W.; Dunlap, B. I.; Carter, C. T. *Phys. Rev. Lett.* **1992**, *68*, 631.
(10) Hamada, N.; Sawada, S.; Oshiyama, A. *Phys. Rev. Lett.* **1992**, *68*, 1579.
(11) Iijima, S. *Nature* **1991**, *354*, 56.
(12) Iijima, S.; Ichihashi, T. *Nature* **1993**, *363*, 603.
(13) Ge, M.; Sattler, K. *Science* **1993**, *260*, 515.
(14) Wildoer, J. W. G.; Venema, L. C.; Rinzler, A. G.; Smalley, R. E.; Dekker, C. *Nature* **1998**, *391*, 59.
(15) Odom, T.; Huang, J.; Kim, P.; Lieber, C. *Nature* **1998**, *391*, 62.
(16) Dresselhaus, M. S.; Dresselhaus, G.; Sugihara, K.; Spain, I. L.; Goldberg, H. A. *Graphite Fibers and Filaments*; Springer-Verlag: New York, 1988.
(17) Bethune, D. S.; Kiang, C. H.; de Vries, M. S.; Gorman, G.; Savoy, R.; Vazquez, J.; Beyers, R. *Nature* **1993**, *363*, 605.
(18) Thess, A.; Lee, R.; Nikolaev, P.; Dai, H.; Petit, P.; Robert, J.; Xu, C.; Lee, Y. H.; Kim, S. G.; Rinzler, A. G.; Colbert, D. T.; Scuseria, G. E.; Tomanek, D.; Fischer, J. E.; Smalley, R. E. *Science* **1996**, *273*, 483.
(19) Journet, C.; Maser, W. K.; Bernier, P.; Loiseau, A.; Lamy de la Chappelle, M.; Lefrant, S.; Deniard, P.; Lee, R.; Fischer, J. E. *Nature* **1997**, *388*, 756.
(20) Charlier, J.-C.; Gonze, X.; Michenaud, J.-P. *Europhys. Lett.* **1995**, *29*, 43.
(21) Olk, C. H.; Heremans, J. P. *J. Mater. Res.* **1994**, *9*, 259.
(22) Carroll, D. L.; Redlich, P.; Ajayan, P. M.; Charlier, J.-C.; Blase, X.; De Vita, A.; Car, R. *Phys. Rev. Lett.* **1997**, *78*, 2811.
(23) Carroll, D. L.; Blase, X.; Charlier, J.-C.; Curran, S.; Redlich, Ph.; Ajayan, P. M.; Roth, S.; Rühle, M. *Phys. Rev. Lett.* **1998**, *81*, 2332.
(24) Rao, A. M.; Richter, E.; Bandow, S.; Chase, B.; Eklund, P. C.; Williams, K. A.; Fang, S.; Subbaswamy, K. R.; Menon, M.; Thess, A.; Smalley, R. E.; Dresselhaus, G.; Dresselhaus, M. S. *Science* **1997**, *275*, 187.
(25) Bandow, S.; Asaka, S.; Saito, Y.; Rao, A. M.; Grigorian, L.; Richter, E.; Eklund, P. C. *Phys. Rev. Lett.* **1998**, *80*, 3779.
(26) Sugano, M.; Kasuya, A.; Tohji, K.; Saito, Y.; Nishina. *Chem. Phys. Lett.* **1998**, *292*, 575.
(27) Ebbesen, T. W.; Ajayan, P. M. *Nature* **1992**, *358*, 220.
(28) Bacon, R. *J. Appl. Phys.* **1960**, *31*, 283.
(29) Krätschmer, W.; Lamb, L. D.; Fostiropoulos, K.; Huffman, D. R. *Nature* **1990**, *347*, 354.
(30) Gamaly, E. G.; Ebbesen, T. W. *Phys. Rev. B* **1995**, *52*, 2083.
(31) Colbert, D. T.; Zhang, J.; McClure, S. M.; Nikolaev, P.; Chen, Z.; Hafner, J. H.; Owens, D. W.; Kotula, P. G.; Carter, C. B.; Weaver, J. H.; Rinzler, A. G.; Smalley, R. E. *Science* **1994**, *266*, 1218.
(32) Amelinckx, S.; Zhang, X. B.; Bernaerts, D.; Zhang, X. F.; Ivanov, V.; Nagy, J. B. *Science* **1994**, *265*, 635.
(33) Snyder, C. E.; Mandeville, H. W.; Tennet, H. G. International Patent WO 89/07163, 1989.
(34) Li, W. Z.; Xie, S. S.; Qian, L. X.; Chang, B. H.; Zou, B. S.; Zhou, W. Y.; Zhao, R. A.; Wang, G. *Science* **1996**, *274*, 1701.
(35) Terrones, M.; Grobert, N.; Olivares, J.; Zhang, J. P.; Terrones, H.; Kordatos, K.; Hsu, W. K.; Hare, J. P.; Townshend, P. D.; Prassides, K.; Cheetham, A. K.; Kroto, H. W. *Nature* **1997**, *388*, 52.
(36) Che, G.; Lakshmi, B. B.; Fisher, E. R.; Martin, C. R. *Nature* **1998**, *393*, 346.
(37) Chen, Y.; Guo, L. P.; Patel, S.; Ye, Y.; Shaw, D. T. *Appl. Phys. Lett.* **1998**, *73*, 2119.
(38) Dai, H.; Rinzler, A. G.; Nikolaev, P.; Thess, A.; Colbert, D. T.; Smalley, R. E. *Chem. Phys. Lett.* **1996**, *260*, 471.
(39) Kong, J.; Soh, H. T.; Cassel, A. M.; Quate, C. F.; Dai, H. *Nature* **1998**, *395*, 878.
(40) Duesberg, G. S.; Burghard, M.; Muster, J.; Phillip, G.; Roth, S. *Chem. Commun.* **1998**, 435.
(41) Tohji, K.; Takahashi, H.; Shinoda, Y.; Shimizu, N.; Jeyadevan, B.; Matsuoka, I.; Saito, Y.; Kasuya, A.; Ito, S.; Nishina, Y. *J. Phys. Chem. B* **1997**, *101*, 1974.
(42) Bandow, S.; Williams, K. A.; Thess, A.; Smalley, R. E.; Eklund, P. C. *J. Phys. Chem. B* **1997**, *101*, 8839.
(43) Liu, J.; Rinzler, A. G.; Dai, H.; Hafner, J. H.; Bradley, R. K.; Boul, P. J.; Lu, A.; Iverson, T.; Shelimov, K.; Huffman, C. B.; Rodriguez-Macias, F.; Shon, Y.; Lee, T. R.; Colbert, D. T.; Smalley, R. E. *Science* **1998**, *280*, 1253.
(44) Ebbesen, T. W.; Ajayan, P. M.; Hiura, H.; Tanigaki, K. *Nature* **1993**, *367*, 519.
(45) Hiura, H.; Ebbesen, T. W.; Tanigaki, K. *Adv. Mater.* **1995**, *7*, 275.
(46) Lu, K. L.; Lago, R. M.; Yu, K. C.; Green, M. L. H.; Harris, P. J. F. *Carbon* **1996**, *34*, 814.
(47) Chen, J.; Hamon, M. A.; Hu, H.; Chen, Y.; Rao, A. M.; Eklund, P. C.; Haddon, R. C. *Science* **1998**, *282*, 95.
(48) Maiti, A.; Brabec, C. J.; Roland, C. M.; Bernholc, J. *Phys. Rev. Lett.* **1994**, *73*, 2468.
(49) Charlier, J.-C.; DeVita, A.; Blase, X.; Car, R. *Science* **1997**, *275*, 646.
(50) Kwon, Y. K.; Lee, Y. H.; Kim, S. G.; Jund, P.; Tomanek, D.; Smalley, R. E. *Phys. Rev. Lett.* **1997**, *79*, 2065.
(51) Haddon, R. C.; Scuseria, G. E., Smalley, R. E. *Chem. Phys. Lett.* **1997**, *272*, 38.
(52) Langer, L.; Bayot, V.; Grivei, E.; Issi, J.-P.; Heremans, J. P.; Olk, C. H.; Stockman, L.; Van Haesendonck, C.; Bruynseraede, Y. *Phys. Rev. Lett.* **1996**, *76*, 479.
(53) Ebbesen, T. W.; Lezec, H.; Hiura, H.; Bennett, J. W.; Ghaemi, H. F.; Thio, T. *Nature* **1996**, *382*, 54.
(54) Kasumov, A. Yu; Khodos, I. I.; Ajayan, P. M.; Colliex, C. *Europhys. Lett.* **1996**, *34*, 429.
(55) Frank, S.; Poncharal, P.; Wang, Z. L.; de Heer, W. A. *Science* **1998**, *280*, 1744.
(56) Batchtold, A.; Strunk, C.; Salvetat, J. P.; Bonard, J. M.; Forro, L.; Nussbaumer, T.; Schonenberger, C. *Nature* **1999**, *397*, 673.
(57) Tans, S. J.; Devoret, M. H.; Dai, H.; Thess, A.; Smalley, R. E.; Geerlings, L. J.; Dekker: C. *Nature* **1997**, *386*, 474.
(58) White, C. T.; Todorov, T. N. *Nature* **1998**, *393*, 240.
(59) Bockrath, M.; Cobden, D. H.; Lu, J.; Rinzler, A. G.; Smalley, R. E.; Balents, L.; McEuen, P. L. *Nature* **1999**, *397*, 598.
(60) Rao, A. M.; Eklund, P. C.; Bandow, S.; Thess, A.; Smalley, R. E. *Nature* **1997**, *388*, 257.
(61) Lee, R. S.; Kim, H. J.; Fischer, J. E.; Thess, A.; Smalley, R. E. *Nature* **1997**, *388*, 255.

(62) Overney, G.; Zhong, W.; Tomanek, D. *Z. Phys. D* **1993**, *27*, 93.
(63) Yakabson, B. I.; Brabec, C. J.; Bernholc, J. *Phys. Rev. Lett.* **1996**, *76*, 2511.
(64) Treacy, M. M. J.; Ebbesen, T. W.; Gibson, J. M. *Nature* **1996**, *381*, 678.
(65) Wong, E. W.; Sheehan, P. E.; Lieber, C. M. *Science* **1997**, *277*, 1971.
(66) Falvo, M. R.; Clary, C. J.; Taylor, R. M.; Chi, V.; Brooks, F. P.; Washburn, S.; Superfine, R. *Nature* **1997**, *389*, 582.
(67) Falvo, M. R.; Taylor, R. M.; Helser, A.; Chi, V.; Brooks, F. P.; Washburn, S.; Superfine, R. *Nature* **1999**, *397*, 236.
(68) Ruoff, R. S.; Lorents, D. C. *Carbon* **1995**, *33*, 925.
(69) Yakabson, B. I.; Brabec, C. J.; Bernholc, J. *J. Comput. Aided Mater. Des.* **1996**, *3*, 173.
(70) Stone, A. J.; Wales, D. J. *Chem. Phys. Lett.* **1986**, *128*, 501.
(71) Yakabson, B. I. *Appl. Phys. Lett.* **1998**, *72*, 918.
(72) Ajayan, P. M.; Ebbesen, T. W.; Ichihashi, T.; Iijima, S.; Tanigaki, K.; Hiura, H. *Nature* **1993**, *362*, 522.
(73) Tsang, S. C.; Harris, P. J. F.; Green, M. L. H. *Nature* **1993**, *362*, 520.
(74) Britto, P. J.; Santhanam, K. S. V.; Alonso, V.; Rubio, A.; Ajayan, P. M. *Adv. Mater.* **1998**, *11*, 154.
(75) Pederson, M. R.; Broughton, J. Q. *Phys. Rev. Lett.* **1992**, *69*, 2689.
(76) Ajayan, P. M.; Iijima, S. *Nature* **1993**, *361*, 333.
(77) Dujardin, E.; Ebbesen, T. W.; Hiura, H.; Tanigaki, K. *Science* **1994**, *265*, 1850.
(78) Tsang, S. C.; Chen, Y. K.; Harris, P. J. F.; Green, M. L. H. *Nature* **1994**, *372*, 159.
(79) Tans, S. J.; Verschueren, A. R. M.; Dekker, C. *Nature* **1998**, *393*, 49.
(80) Crespi, V. H.; Cohen, M. L.; Rubio, A. *Phys. Rev. Lett.* **1997**, *79*, 2093.
(81) Wagner, H. D.; Lourie, O.; Feldman, Y.; Tenne, R. *Appl. Phys. Lett.* **1998**, *72*, 188.
(82) Schadler, L. S.; Giannaris, S. C.; Ajayan, P. M. *Appl. Phys. Lett.* Submitted.
(83) Curran, S.; Ajayan, P. M.; Blau, W.; Carroll, D.; Coleman, J.; Dalton, A.; Davey, A. P.; McCarthy, B.; Strevens, A. *Adv. Mater.* In press.
(84) Dai, H. J.; Hafner, J. H.; Rinzler, A. G.; Colbert, D. T.; Smalley, R. E. *Nature* **1996**, *384*, 147.
(85) Dai, H.; Franklin, N.; Han, J. *Appl. Phys. Lett.* **1998**, *73*, 1508.
(86) Wong, S. S.; Joselevich, E.; Woolley, A. T.; Cheung, C. L.; Lieber, C. M. *Nature* **1998**, *394*, 52.
(87) de Heer, W. A.; Chatelain, A.; Ugarte, D. *Science* **1995**, *270*, 1179.
(88) Fan, S.; Chapline, M. G.; Franklin, N. R.; Tombler, T. W.; Cassell, A. M.; Dai, H. *Science* **1999**, *283*, 512.
(89) Britto, P. J.; Santhanam, K. S. V.; Ajayan, P. M. *Bioelectrochem. Bioenerg.* **1996**, *41*, 121.
(90) Planeix, J. M.; Coustel, N.; Coq, B.; Brotons, V.; Kumbhar, P. S.; Dutartre, R.; Geneste, P.; Bernier, P.; Ajayan, P. M. *J. Am. Chem. Soc.* **1994**, *116*, 7935.
(91) Niu, C.; Sichel, E. K.; Hoch, R.; Moy, D.; Tennet, H. *Appl. Phys. Lett.* **1997**, *7*, 1480.
(92) Dillon, A. C.; Jones, K. M.; Bekkedahl, T. A.; Kiang, C. H.; Bethune, D. S.; Heben, M. J. *Nature* **1997**, *386*, 377.
(93) Special Issue on Carbon Nanotubes, *Carbon* **1995**, *33*, 873−1006.
(94) Special Issue on Carbon Nanotubes, *Applied Physics A* **1998**, Volume 67.

CR970102G